



NUMERICAL MODEL FOR BUCKLING RESTRAINED BRACES USING AN ALTERNATIVE CONFINING MATERIAL

M. Morral⁽¹⁾, R. Herrera⁽²⁾, J. Beltrán⁽³⁾, M.O. Moroni⁽⁴⁾, M. Murillo⁽⁵⁾

⁽¹⁾ Graduate student, Dept. of Civil Engineering, University of Chile, Santiago, Chile, mmorral@ing.uchile.cl

⁽²⁾ Assistant Professor, Dept. of Civil Engineering, University of Chile, Santiago, Chile, riherrer@ing.uchile.cl

⁽³⁾ Assistant Professor, Dept. of Civil Engineering, University of Chile, Santiago, Chile, jbeltran@ing.uchile.cl

⁽⁴⁾ Associate Professor, Dept. of Civil Engineering, University of Chile, Santiago, Chile, mmoroni@ing.uchile.cl

⁽⁵⁾ Graduate student, Dept. of Civil Engineering, University of Chile, Santiago, Chile, mmurillo@ug.uchile.cl

...

Abstract

Buckling restrained braces are metallic dissipators made up of a core of ductile steel, designed to resist similar tensile and compressive forces, by confining the core and preventing global and local buckling. Generally, mortar is used as confining material.

The main objective of this research is to determine the properties required of an alternative material to be used as confining material in a BRB and to predict analytically the behavior of the brace subjected to cyclic loads.

First, a model that represents the behavior of a beam on an elastic foundation was used to determine the Euler's critical BRB buckling load and the required value of shear modulus G of the material, in order to restrict buckling of the steel core made of different commercial plates.

Next, a 3D finite element model was developed with ANSYS 15.0 software which considers geometric non-linearity, and nonlinear materials and contacts. An isotropic hardening law was used for the steel core model. In order to validate the model, cycles from available experimental data of BRB filled with mortar were compared with the numerical results. A significantly larger maximum strength and asymmetric compression hardening are predicted by the model with respect to the experimental results. This effect is minimized when a softer material is used.

A parametric analysis for different values of shear and bulk moduli, friction between the steel core and the confining material and the confined length of the device was performed. Monotonic and cyclic displacements of increasing amplitude were applied to the model and cycles and critical buckling loads were determined. This analysis allowed to identify the influence of the main variables on the stress distribution and the level of confinement, and to predict the critical buckling loads

Keywords: Buckling Restrained Brace; elastomers; metallic dissipators; numerical finite element model

1. Introduction

Conventional braces present stiffness and strength degradation due to buckling effects when subjected to compression, reducing its capacity to dissipate energy. In contrast, buckling restrained braces (BRB) prevent elastic buckling at low compression modes, allowing the brace to yield in both tension and compression (higher modes) due to the confinement of the steel core avoiding local and global buckling of the brace. This produces a stable hysteretic behavior substantially equal in tension and compression (Fig. 1).

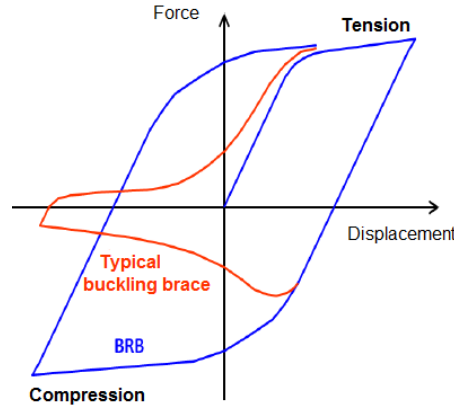


Fig. 1: Conventional and BRB behavior

Therefore, replacing conventional braces by BRB allows the structure to develop a significant amount of inelastic deformation when subjected to seismic forces. The inelastic deformation can be limited to the yielding of the BRB steel core, while beams, columns and connections remain within their elastic range minimizing the potential damage.

BRBs are basically composed of three main parts (Fig. 2):

- Steel core, designed to resist tension and compression loads.
- Debonding material, its function is to allow the core to slide freely within the confinement and the lateral expansion of the core (Poisson effect) when it is under compression load.
- Confining material, designed to prevent global and local elastic buckling of the core. The core is placed inside a steel casing filled with a confining material as concrete.



Fig. 1: BRB General description [1]

The main objective of this research is to determine the properties required of an alternative material to be used as confining material in a BRB and to predict analytically the behavior of the brace subjected to cyclic loads. This is performed using analytical and numerical procedures.

2. Analytical Procedure

Black et al [2] determined an analytical solution to describe the BRB behavior, based on a model that represents the behavior of a beam on an elastic foundation, that can be used to determine the Euler's critical BRB buckling load and the required value of shear modulus G of the material, in order to restrict local and global buckling of the steel core. The material is considered elastic, linear and isotropic. The required shear modulus determines the range of materials that can be used in the numerical model.

For a brace with buckling length L , the critical buckling load, Eq. (1), is just the sum of the critical load of the confining material and the casing. Therefore, the overall stability of a buckling restrained brace is guaranteed when the Euler buckling load P_{cr} exceeds the core ultimate load $P_u = \sigma_u A_{core}$.

$$P_{cr} = P_e = \frac{\pi^2}{(KL)^2} (E_i I_i + E_o I_o) \quad (1)$$

On the other hand, assuming that the material confinement reaction forces can be approximated by a curve similar to the steel core transverse deflection, $y(x)$, the load exerted along the steel core can be expressed by $q(x) = \beta y(x)$, where β is the distributed stiffness per unit area and $y(x)$ is obtained from Eq. (2).

$$E_i I_i \frac{d^4 y(x)}{dx^4} + P \frac{d^2 y(x)}{dx^2} + \beta y(x) = 0 \quad (2)$$

The solution to Eq. (2) shows that the critical buckling load of the inner core in the higher modes is independent of the boundary conditions at the ends and it depends only on the stiffness per unit area of the confining material and core geometric properties, $P_{cr} = \sqrt{\beta E_i I_i}$.

As stated previously, in order to prevent buckling of the inner core in the lower modes, the critical Euler buckling load must be greater than or equal to the ultimate load of the steel core, which requires

$$\beta \geq \frac{\sigma_u^2 A_i^2}{4 E_i I_i} \quad (3)$$

Where E_i is the modulus of elasticity used to obtain the required stiffness to prevent buckling of the steel core in lower modes. Because it occurs in the plastic range, the tangent elastic modulus E_t must be used.

2.1 Required stiffness of the confining material

Using the Generalized Lamé-Hooke law, the material elastic stiffness β_e is obtained, considering as boundary conditions the presence of the steel tube that impedes lateral displacement. It depends on the elastic modulus E_c and Poisson's ratio ν of the material, Eq. (4). β_e should be equal or greater than β for the material to be effective in restraining buckling of the core.

$$\beta_e = E_c \frac{1-\nu}{(1+\nu)(1-2\nu)} \quad (4)$$

Using the relationship between the elasticity variables of an elastic, linear and isotropic material, Eq. (5) gives the required material shear modulus in order to prevent buckling of the brace.

$$G = \frac{E_c}{2(1+\nu)} \quad (5)$$

Table 1 presents the required stiffness for different commercial ASTM A36 plates, and Table 2 the required properties of the material calculated using Eq. (4) and (5).

Table 1 - Required stiffness to avoid core buckling

B (mm)	t (mm)	Weight (kg/m)	β (GPa)
100	6	4.71	7.3
	8	6.28	5.5
	10	7.85	4.4
	11	8.64	4.0
	12	9.42	3.6

Table 2 - Required material properties

E (MPa)	206 - 429
ν	0.49
G (MPa)	70 - 144
β (GPa)	3.6 - 7.3

3. Numerical Procedure

A 3D finite element model was developed with ANSYS 15.0 software which considers geometric non-linearity, and nonlinear materials and contacts. An isotropic hardening law was used for the steel core model. The steel core is a rectangular plate 100x10 mm confined by an elastoplastic material which is encased by a square steel jacket, 200x200x5mm.

First, the buckling modes of the steel core were determined. The deformed buckling shape was used to generate an initial imperfection of 3 mm amplitude, to induce buckling of the core when the BRB is subjected to an axial compressive load. Subsequently, the BRB model was subjected to monotonic and cyclic loads varying the properties of the confining material.

3.1 Material properties

ASTM A36 with yield stress $F_y = 250$ MPa, ultimate stress $F_u = 460$ MPa, modulus of elasticity $E = 200$ GPa and tangent modulus $E_t = 1450$ MPa, was used for both the core and the casing.

A hyper elastic material from ANSYS 15 library was used to model the confining material. It uses the "Neo-Hookean" model to represent the non-linear stress-strain behavior of materials subjected to large deformations. The Neo-Hookean model determines the stress-strain relationship using the strain energy density W which depends on the initial shear module G_0 , the incompressibility parameter $d=1/k$, the first invariant of the stress tensor and the determinant of the elastic deformation gradient as it is shown in Eq. (6).

$$W = \frac{G_0}{2} (\bar{J}_1 - 3) + \frac{K}{2} (J - 1)^2 \quad (6)$$

3.2 Boundary and contact conditions

A frictional contact was considered between the steel core and the confining material, allowing a relative displacement controlled by a friction coefficient equal to 0.1 for the case where the adherence is small and 0.5 when the adherence is large. A bonded contact between the outer jacket and the confining material was considered, so relative displacement between both elements was not allowed.

With respect to the boundary conditions, the steel core was fixed at one end and with a roller at the other end. The steel core is subjected to tension and compression load, while the confining material is only restricted by its contact with the plate, and the steel casing is restricted by its contact with the confining material.

3.3 Numerical model validation

Results from experimental test performed by Newell et al [3] were used to validate the numerical finite element model. A shape similar to the first buckling mode with maximum amplitude of 3 mm was assumed as initial imperfection. A friction coefficient $\nu = 0.1$ was used between the steel core and the confining mortar.

The BRB was subjected to the same displacement protocol; however, in order to reduce computational costs, the first section was reduced to only one cycle, since it corresponds to the elastic range and only 4 displacements amplitudes were considered subsequently.

Fig. 3 shows that maximum numerical forces both in tension and compression are larger than those obtained experimentally while the displacements are smaller, which implies that the numerical model is stiffer than the experiment. Three relevant phenomena can be seen in the numerical model: (1) significant increase in tension and compression strength; (2) increase in axial stiffness of BRB and (3) asymmetric compression hardening.

The increase in tensile and compressive stresses is related to the isotropic hardening imposed on the model, which is characterized by the expansion of the yield surface at every cycle, so an increase in yield stress in one direction involves the same increase in the opposite direction.

The main reason behind the compression hardening is the interaction between the steel core and the confining concrete. The core buckles inside the concrete, deforming it locally, which generates interlocking between the core and the concrete, in addition to the friction. Therefore, a larger portion of the axial load is

transferred to the concrete, stiffening the BRB; this phenomenon has been reported by Zsarnoczay [4]. Fig. 4 shows the normal stresses in the concrete in the longitudinal direction once the steel core starts to buckle, increasing the BRB stiffness in compression. This effect can be quantified by comparing the plate axial stiffness AE/L (234 kN/mm) with the elastic stiffness from the numerical model (471 kN/mm) and the experiment (357 kN/mm). The numerical model is 30% stiffer than the experiment.

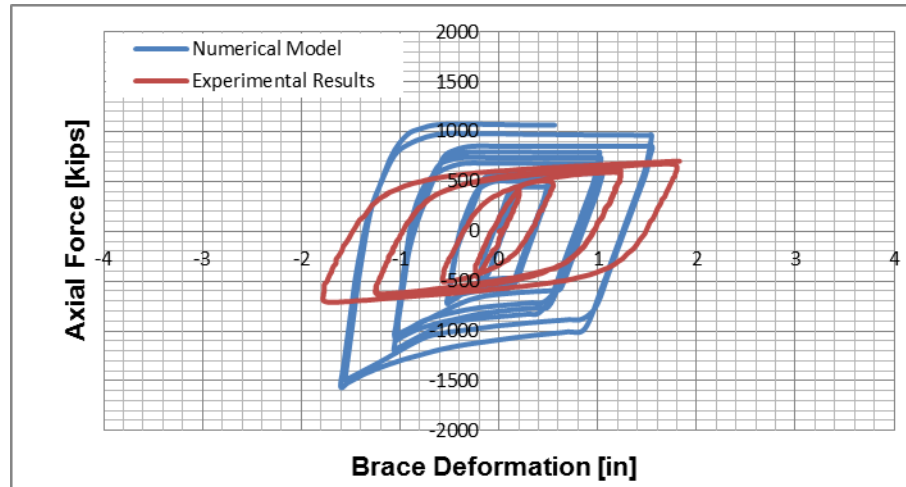


Fig.1: P vs Δ curve, numerical model v/s experimental results

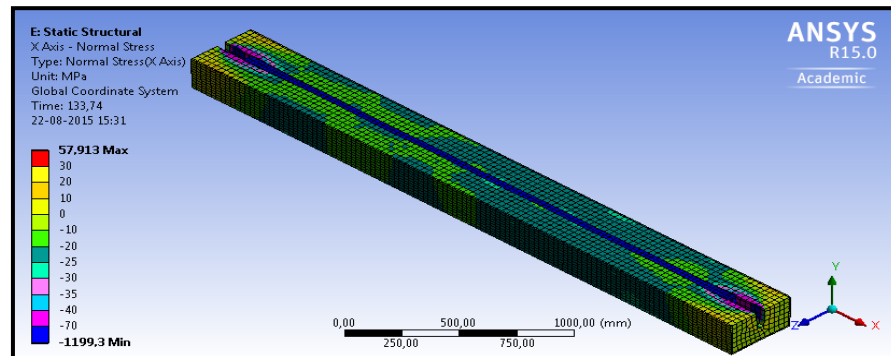


Fig.4: Normal stresses in BRB longitudinal direction

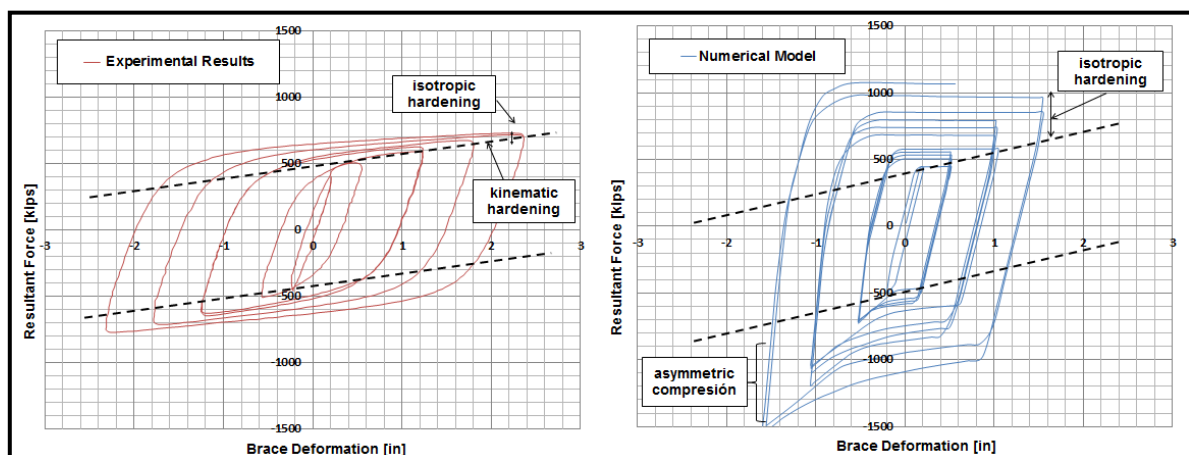


Fig. 5: Hysteretic behavior experimental test and numerical model

Additionally, in the experiment, the BRB presents a combination of kinematic and isotropic hardening, because the hysteresis loop has not only a slight expansion of the yield surface, but also presents a displacement of it, which is responsible for a decrease in yield stress in the opposite direction after an increase in yield stress occurs due to hardening. This combined behavior prevents excessive strength increase in both tension and compression and generates hysteresis loops with a non-zero post yielding stiffness (Fig. 5).

Therefore, the numerical model is not able to fully predict the behavior of the BRB. However, the results presented below will be conservative in terms of the maximum forces expected in the brace and it is expected that the asymmetrical compression effect will be reduced when using a softer confining material, as is the case in this research.

4. Alternative confining material

To predict the behavior of a buckling restrained brace confined by an alternative elastoplastic material, different cases were studied considering four variables of interest; (i) friction coefficient μ to study the adherence between the core and confining material; (ii) shear modulus G ; (iii) Bulk modulus κ to study the confining capacity of the alternative material; and (iv) confined length L_c . Twenty four different models were analyzed subjected to cyclic loads by modifying the four variables considered, while twelve models were analyzed subjected to monotonic loads, for which L_c is not a relevant variable.

4.1 Volumetric and shear modulus

The shear modulus G and bulk modulus κ are proportional to the strain energy per unit volume of the confining material, which implies that for larger G or κ , the strain energy per unit volume will increase and thus a greater compression load will be resisted by the confining material. As the lateral stiffness and the compression strength of the confining material directly affect the stability of the BRB core, a greater ductility and BRB strength is attained as the shear or bulk modulus increase.

When the shear modulus is about 100 [MPa], the steel core does not buckle, independently of the κ value. But for smaller G , a larger bulk modulus is required to avoid premature buckling failure. When $G = 50$ [MPa], κ must be 2000 [MPa] in order to prevent the premature buckling of the BRB (Fig 6).

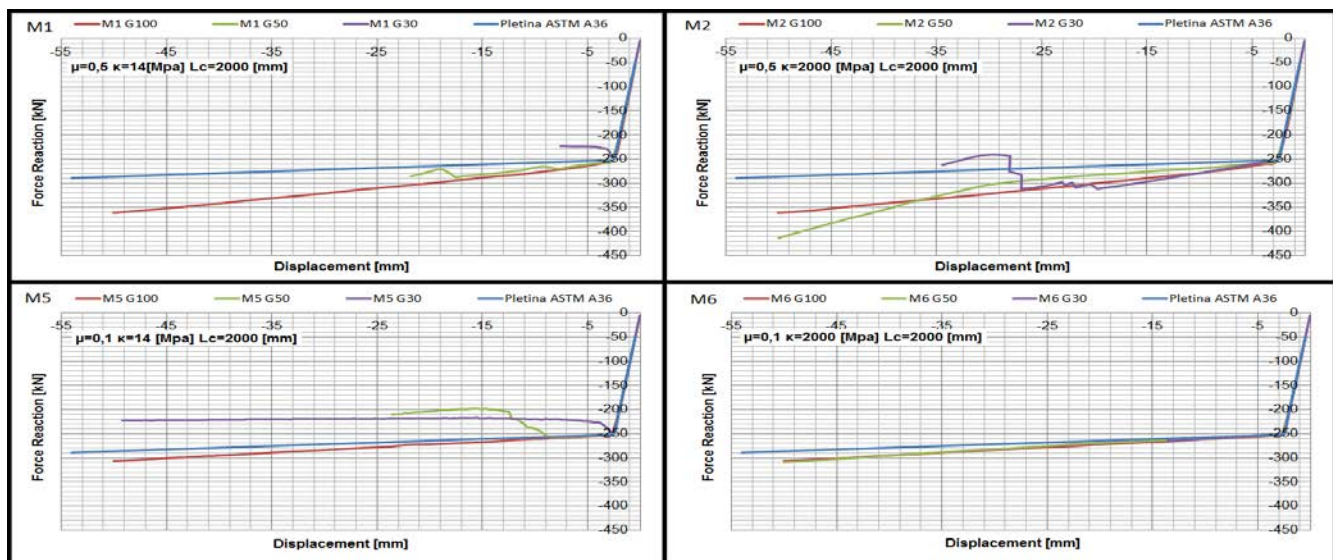


Fig. 6: Effect of G and κ variation, Monotonic loading

4.2 Friction coefficient

The friction coefficient controls the displacement compatibility between the steel core and the confining material, so for larger μ , the relative displacements are lower and the transferred stresses are larger. This effect is shown in Fig.7. In addition, when the compression load increases, the steel core lateral displacements produce an increment in the normal forces that are transferred to the confining material, increasing in turn the friction, which may explain the asymmetric behavior in the hysteresis cycle of the confining material and thereby the slight increase in compressive strength.

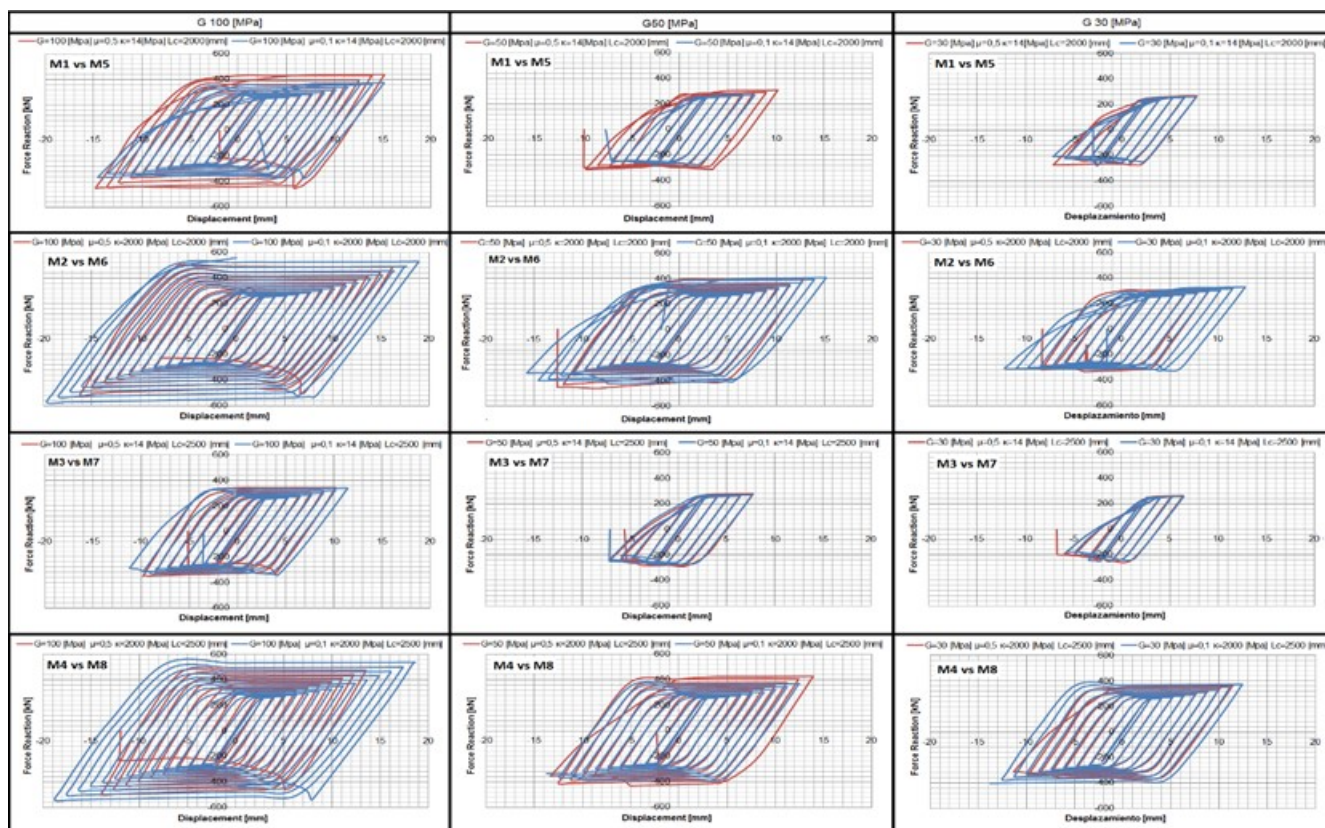


Fig. 7: Hysteresis cycle for different μ values

4.3 Confined length

During cyclic loading, the core yields in tension becoming longer. Depending on the amount of permanent elongation, the core may buckle outside the confined region. To study this phenomenon, two different confined lengths were considered to prevent failures outside the confined zone and to ensure a homogeneous core confinement for the cyclic analyses. However, in most cases the achieved ductility did not vary. Fig. 8 shows that the elastic slope both in tension and compression increases when the length of confinement, L_c , increases.

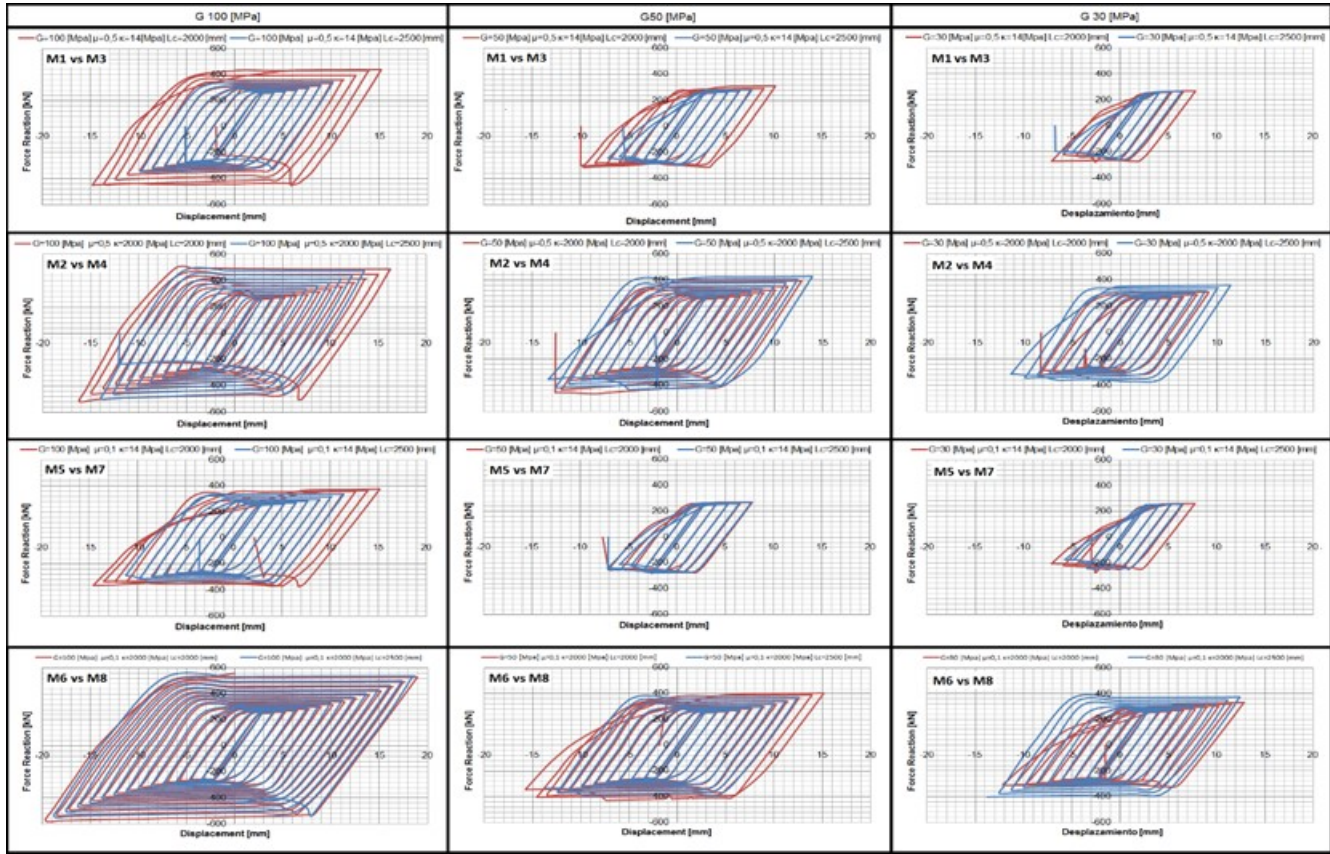


Fig. 8: Hysteresis cycles for different L_c values

4.4 Cyclic behavior

The isotropic hardening law used in the numerical model, generates a stiffer BRB with higher strength both in tension and compression. The asymmetry of the hysteresis loop is attenuated when a softer material is used.

Fig. 9 shows the maximum longitudinal compression stress distribution in the steel core, the confining material and the casing for $G = 50$ MPa. The steel core yields in compression and deforms in the plastic range. Some out of plane buckling occurs in a limited region inside the confinement, but it is restricted by the confining material. Some forces are transmitted to the confining material and the casing through friction, but both remain elastic.

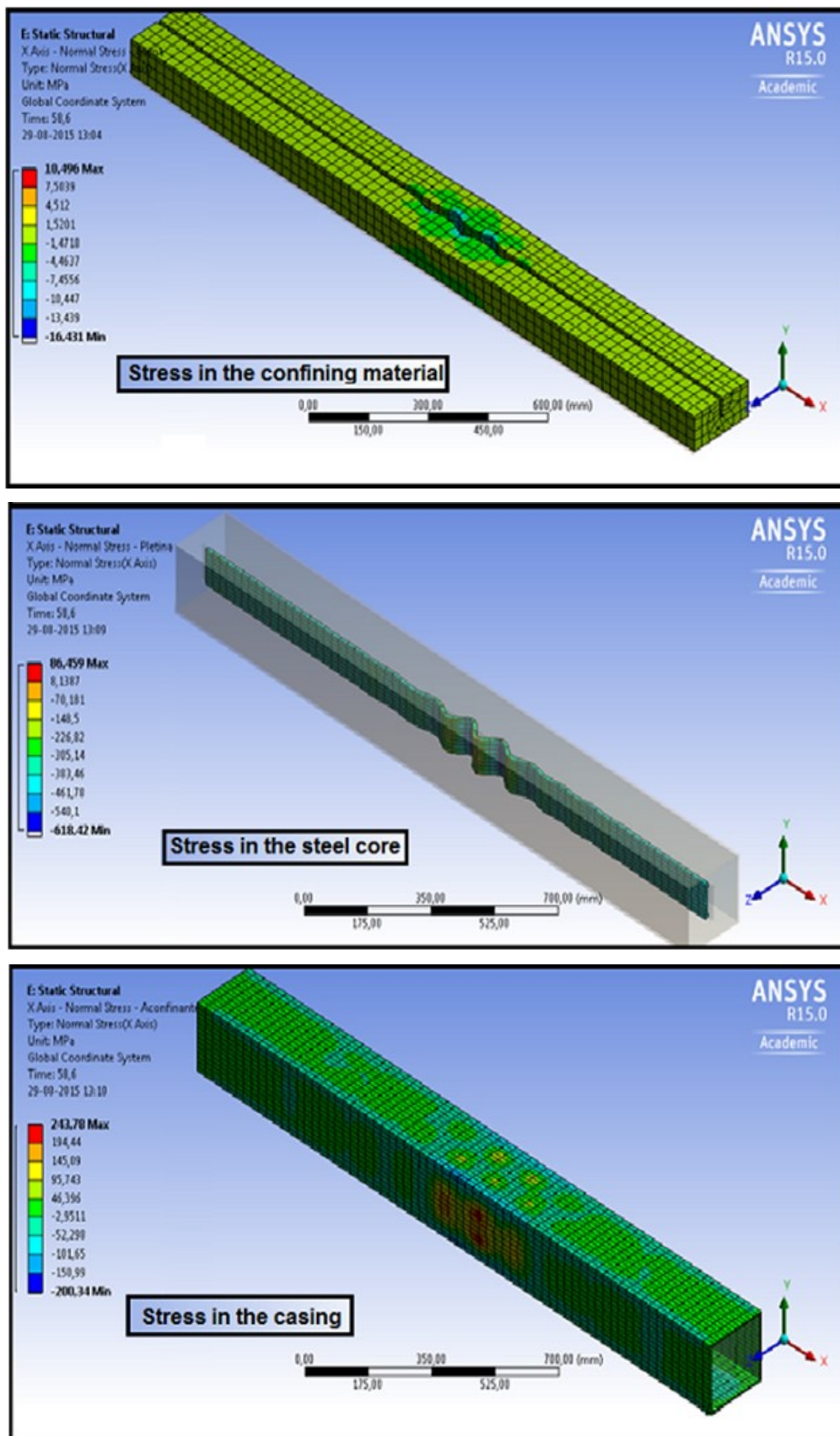


Fig. 9: Compression stress distribution

Fig. 10 shows the maximum longitudinal tensile stress distribution in the steel core, the confining material, and the casing for the same BRB. The steel core also yields tension and deforms in the plastic range. The stresses in the confining material are negligible, showing that slip occurs between the steel core and the confining material.

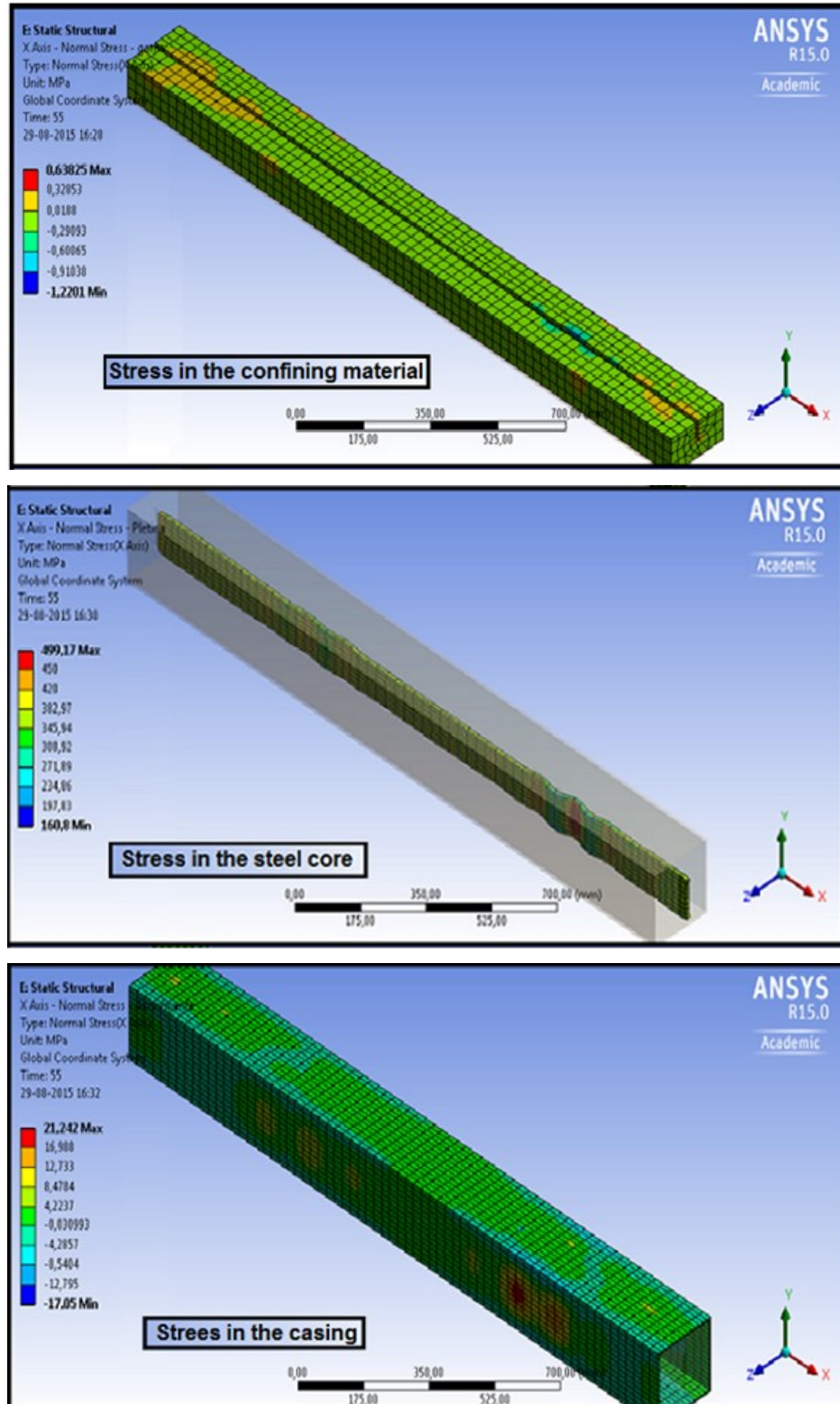


Fig. 10: Tensile stress distribution

Fig. 11 shows failure that occurs due to local buckling of the steel core in one of its ends for compressive stress around 420 [MPa]. In order to prevent local buckling near the ends of the plate, where confinement is lower, a larger confined length was used. However, the numerical results indicate that the stiffness of the confining material is unable to prevent local buckling in the plate. Therefore, the steel core must be stiffened near the ends to prevent this failure.

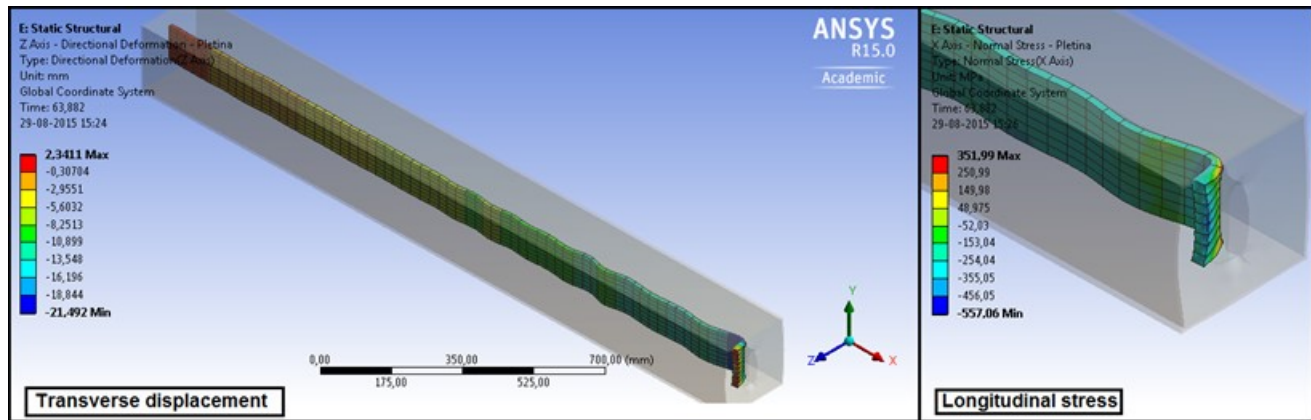


Fig. 11: Failure mode

4.5 Comparison between analytical and numerical results

To determine the properties of the confining material to avoid BRB local and global buckling both an analytical solution and a numerical finite element model of BRB have been used. For the commercial plates considered the value of shear modulus calculated analytically varies between 36 and 144 [MPa]. The numerical model requires a shear modulus equal to 100[MPa].

The theoretical Euler buckling load of the confined steel core considered in the numerical model is 352 [kN], equivalent to a stress of 352 [MPa]. However, the numerical model predicts that local buckling occurs at 426 [kN] equivalent to a stress of 426 [MPa]. This difference can be attributed to consider a linear elastic material to determine the shear modulus of the confining material. On the other hand, the increase in maximum strength due to isotropic hardening can also be an explanation for this difference.

5. Conclusions

The main objective of this research was to study the behavior of BRB subjected to cyclic loads, using an alternative elastoplastic confining material using analytical and numerical procedures.

The analytical solution to the BRB instability problem under compression and the Generalized Lamé-Hooke law, allowed to determine the Euler critical buckling load of the confined steel core and to obtain similar values for the required shear modulus of the confining material to restrain buckling, between the analytical and the numerical model.

The isotropic hardening law included in the finite element model is not able to completely represent the behavior of BRB. The model predicts larger strength, higher axial stiffness and asymmetric compression hardening. These effects are less pronounced when softer materials are used as confining material. However, the numerical model is useful to identify the main variables that influence the BRB response.

Both the shear modulus and the bulk modulus directly affect the rigidity of the confining material and thereby the core confinement, allowing greater ductility and strength as the shear modulus or bulk modulus increases. The friction coefficient controls the displacement compatibility between the steel core and the confining material; larger μ values, results in lower relative displacements and larger transmitted forces. This effect produces a steepening in post yield curve P vs Δ , increasing the asymmetry of the loop in tension and compression.

Increasing the confined length does not prevent buckling of the steel core at its ends, so it is advisable to consider a larger section in order to increase the stiffness and to prevent buckling in that less confined area.

Important variables to consider regarding convergence of the finite element model are the initial imperfection and the mode shape assumed to induce the steel core buckling. For this purpose, different initial conditions were analyzed, opting for the buckling mode number 10 and a value of 3 [mm] amplitude.

The finite element model developed as part of this research should be considered as a tool to help future design of BRB. This model proved to be complex and computationally expensive due to the nonlinear properties of materials, contacts and large deformation inclusion. However, it would be necessary to consider the effects of kinematic hardening to have a better reproduction of the BRB and a decrease in the strength presented with this the model.

Acknowledgments

Funding by Fondef IDeA grant CA13I10026 and University of Chile is greatly appreciated.

References

- [1] Cancelado R. (2013): Experimental Characterization of Practical Scale Buckling Restrained Braces under Cyclic Testing. *rev.ing. ISSN. 0121-4993*, pp 17-23, Bogota D. C., Colombia.
- [2] Black C, Makris N, Aiken I.D. (2002): Component testing, stability analysis and characterization of buckling-restrained braces. *Technical Report PEER 2014-002/08*. Pacific Earthquake Engineering Research Center, Berkeley, USA.
- [3] Newell J, Uang C. Ming, Benzoni G (2006): Subassemblage Testing of Corebrace Buckling Restrained Braces (G Series). *Technical Report PEER 06/01*. Structural Systems Research Project, University of California, USA.
- [4] Zsarnóczy Á. (2013): Experimental and Numerical Investigation of Buckling Restrained Braced Frames for Eurocode Conform Design Procedure Development, PhD Dissertation, Department of Structural Engineering, Budapest University of Technology and Economics.